

Review

Photophysics in bipyridyl and terpyridyl platinum(II) acetylides[☆]

Felix N. Castellano^{*}, Irina E. Pomestchenko, Elena Shikhova, Fei Hua,
Maria L. Muro, Nepali Rajapakse

Department of Chemistry and Center for Photochemical Sciences, Bowling Green State University, Bowling Green, OH 43403, United States

Received 30 January 2006; accepted 7 March 2006

Available online 17 March 2006

Contents

1. Introduction	1819
2. Synthetic approaches to bipyridyl and terpyridyl platinum(II) acetylides	1819
3. Ground state electronic spectra, electrochemistry, and electronic structure calculations	1820
4. Photoluminescence properties	1821
5. Excited state absorption spectrometry	1825
5.1. Supra-nanosecond spectrometry	1825
5.2. Ultrafast transient absorption spectrometry	1826
6. Concluding remarks	1827
Acknowledgements	1827
References	1827

Abstract

The photophysical properties of mononuclear Pt^{II} chromophores of the general structural formulae: Pt(LL)(C≡CR)₂ and [Pt(LL)(C≡CR)]⁺ (LL = substituted or unsubstituted 2,2'-bipyridine; LLL = substituted or unsubstituted 2,2':6',2''-terpyridine; R = aryl or alkyl) are described. Topics related to their preparation, spectroscopy, photochemistry, and photophysics are reviewed.

© 2006 Elsevier B.V. All rights reserved.

Keywords: Platinum; Photochemistry; Photophysics; Photoluminescence; Transient spectroscopy

1. Introduction

Since the original description of Pt(phen)(C≡CPh)₂ by Che and co-workers in 1994 [1], the number of related square planar platinum(II) acetylides bearing a lone polyimine ligand has enormously expanded. Such molecules have demonstrated promise in diverse applications including optical power limiting [2,3], electroluminescence [4], singlet oxygen photosensitization [5,6], photocatalytic hydrogen production [7], cation sensors [8–10], vapochromism [11], medicinal chemistry [12], and as extrinsic luminescent probes [13]. In general, these chromophores are rich in terms of their photophysics, combining properties of traditional coordination compounds and

organometallics within the same structure. This amalgamation has inspired creativity in molecular design, uncovering new and sometimes unexpected photophysical properties in seemingly straightforward platinum(II) complexes. The current review will limit its focus to the photophysical properties of mononuclear Pt^{II} chromophores bearing a combination of one or more alkyl- or arylacetylide ligands in concert with a lone polyimine (2,2'-bipyridine or 2,2':6',2''-terpyridine) fragment.

2. Synthetic approaches to bipyridyl and terpyridyl platinum(II) acetylides

The syntheses of compounds which are the subject of this review require relatively facile procedures. The synthesis generally departs either directly from K₂PtCl₄ [14] (acidic aqueous reaction conditions) or from Pt(DMSO)₂Cl₂ [15] (organic solvents) where the polyimine ligand displaces appropriate labile ligands, producing the corresponding Pt(LL)Cl₂ or

[☆] ISPPCC 16 contribution.

^{*} Corresponding author. Tel.: +1 4193727513; fax: +1 4193729809.
E-mail address: castell@bgsu.edu (F.N. Castellano).

[Pt(LL)Cl]⁺ species. The introduction of the acetylide unit(s) to the platinum(II) center is readily accomplished through a chloride-to-acetylide metathesis mediated by a CuI catalyst in an organic solvent/base mixture [16,17]. Although this synthetic route has been extensively utilized, a catalyst-free pathway has also been developed for various triflate precursors [10]. In these situations, the terminal acetylene readily couples to the metal center at room temperature, producing the metal–acetylide bond in high yield without the need for the CuI catalyst. The metal–acetylide complexes should not be considered inert as Pt(dbbpy)(C≡CPh)₂ [dbbpy = 4,4′-di(*tert*-butyl)-2,2′-bipyridine] experiences dark oxidative addition chemistry with I₂, producing the six-coordinate Pt(IV) complex [17]. Over periods of days, the Pt(IV) complex undergoes reductive elimination, producing Pt(dbbpy)I₂ and the coupled diacetylene.

3. Ground state electronic spectra, electrochemistry, and electronic structure calculations

Pt(LL)(C≡CR)₂ and [Pt(LL)(C≡CR)]⁺ molecules display characteristic low energy absorption bands that span wavelengths from approximately 350 nm to beyond 600 nm, depending upon the nature of the polyimine and acetylide ligands. In molecules where acetylide-localized $\pi-\pi^*$ transitions reside at high energies, the low energy absorption bands have been proposed to originate predominately from metal-to-ligand charge transfer (MLCT) transitions [4,18–20]. Cyclic voltammetry data generally correlate well with the lowest energy optical transitions, where the first reduction is without question attributed to reduced polyimine ligand and the first oxidation is generally believed to be metal based. The potential of the metal-centered oxidation is extremely sensitive to the nature of the acetylide ligand(s) in both bipyridine and terpyridine structures, oxidation potentials become increasingly negative with increasing σ -donor strength. Unfortunately, the irreversible nature of the first oxidation prohibits precise quantitative analysis and oxidative spectroelectrochemistry at room temperature results in decomposition, at least in every molecule studied to date in our laboratory. The electrochemistry results are easy to understand since any Pt(III) structure produced as a result of oxidation would be unstable with respect to both Pt(II) and Pt(IV). To date the nature of the irreversibly formed oxidation products have not been explored. Therefore, a substantial challenge remains in understanding the nature of the oxidized portion of the molecule and by default the “hole” transiently produced in the charge transfer excited state.

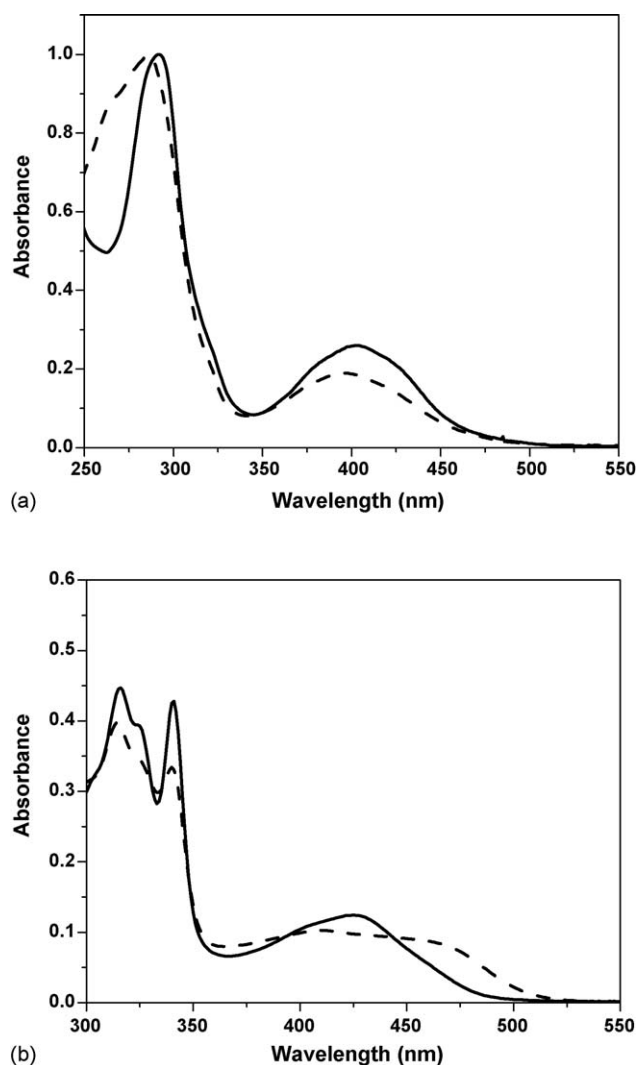
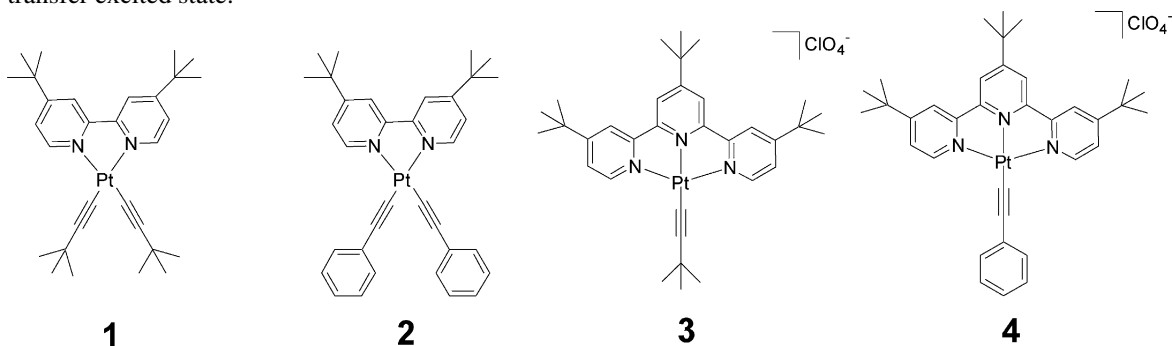


Fig. 1. Absorption spectra of (a) **1** (solid line) and **2** (dashed line) and (b) **3** (solid line) and **4** (dashed line) in CH₂Cl₂.

Many experimentalists have realized that the nature of the acetylide ligand(s) greatly influences the energy, width, and bandshape of the charge transfer transitions in these molecules, particularly noticeable in the terpyridyl structures [20,21]. To illustrate important similarities and differences, Fig. 1 presents the absorption spectra of four closely related Pt(dbbpy)(C≡CR)₂ (**1** and **2**) and [Pt(*t*Bu₃tpy)(C≡CR)]⁺ (**3** and **4**) [*t*Bu₃tpy = 4,4′,4″-tri(*tert*-butyl)-2,2′:6′,2″-terpyridine];



R = *t*-butyl or phenyl] structures measured in CH₂Cl₂ at room temperature. The σ -donor strengths of *t*-butylacetylide and phenylacetylide are essentially identical [22,23], so one would expect no large energy differences in their respective Pt \rightarrow LL or Pt \rightarrow LLL MLCT transitions. Recent work from our laboratory examined the photophysical properties of three Pt(dbppy)(C \equiv CR)₂ complexes (R = –SiMe₃, –C \equiv C–SiMe₃, –*t*-Bu), making direct comparisons with DFT calculations [22]. This work demonstrated that the HOMO contained substantial contributions from metal d- and acetylide π orbitals while the LUMO was predominately bipyridine localized. The lowest excited state in these molecules was calculated by TD-DFT as primarily HOMO \rightarrow LUMO in nature, largely consistent with a MLCT assignment, although contributions from the acetylide π orbitals cannot be ignored. These calculations also successfully predicted the relative energy positions and separations experimentally observed for the complexes, warranting further application of DFT/TD-DFT in related systems. The similarity of the band profiles and energies observed for the alkyl- and arylacetylide Pt(II) bipyridine complexes in Fig. 1a are reminiscent of that expected for MLCT transitions. In other words, MLCT transition energies measured in the same solvent in these two molecules should be affected by electron density at the metal center and the chromophoric diimine ligand which are identical in the two structures. The former is partially controlled by the σ -donor strength of the acetylide ligands which are known to be almost identical. Therefore the MLCT assignment seems rather appropriate since the phenyl units do not impart additional optical transitions relative to the *t*-butyl structure.

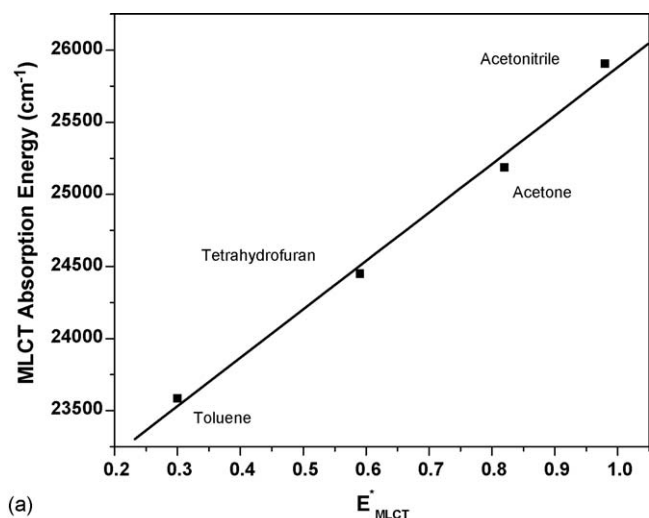
While there are only subtle differences in the charge transfer absorptions associated with the bipyridyl structures (Fig. 1a) the lowest energy features observed in the terpyridyl structures are markedly different (Fig. 1b). The increased bandwidth observed in the phenylacetylide complex **4** indicates the presence of additional electronic transitions of perhaps acetylide-to-terpyridine ligand-to-ligand charge transfer (LLCT) or more appropriately (metal–ligand)-to-ligand charge transfer (ML)LCT. The (ML) designation symbolizes the intimate electronic coupling observed between metal-based d-orbitals and acetylide π -orbitals in these structures. The (ML)LCT assignment (originally presented as MMLL'CT or mixed metal–ligand-to-ligand charge transfer) has been used extensively in describing the charge transfer states of Pt(diimine)(dithiolate) structures, where the dithiolate ligand orbitals are strongly mixed with those of the Pt(II) metal center [24]. Recent electronic structure calculations using DFT and TD-DFT methods yielded data similar to what we have observed in the bipyridine alkylacetylide complexes [25]. In all cases, the acetylide π orbitals play a significant role in the frontier occupied orbitals of the terpyridyl molecules regardless of whether an alkyl- or arylacetylide ligand is present. An interesting facet of these calculations is that the C \equiv CR group contributes substantially to the HOMO density that the lowest energy transition has been described as MLCT/LLCT in character [25], essentially equivalent to the (ML)LCT designation presented above. These considerations are especially important for arylacetylide-containing structures with large π -systems that can significantly contribute electron density in the

highest occupied orbitals. This seems to be the case in **4** where the phenylacetylide orbitals are playing a more significant role which result in the observation of additional optical transitions and concomitant broadening of the absorption spectrum. However, with such strong mixing of metal and ligand orbitals, charge transfer assignments become somewhat ambiguous. This uncertainty has led to debates over which description or admixture (i.e. MLCT, LLCT, or (ML)LCT) most adequately depicts the true situation in the lowest energy transitions in these complexes. While we value precise spectroscopic assignments, an important issue to recognize is that there are opportunities to expand the way we think about intramolecular charge transfer processes in inorganic systems using these molecules. They provide a framework where ancillary ligands actually play a major role in excited state behavior, such as delocalization of the hole over both metal and acetylide ligand, which inevitably leads to transient optical properties distinct from more traditional charge transfer complexes such as [Ru(bpy)₃]²⁺.

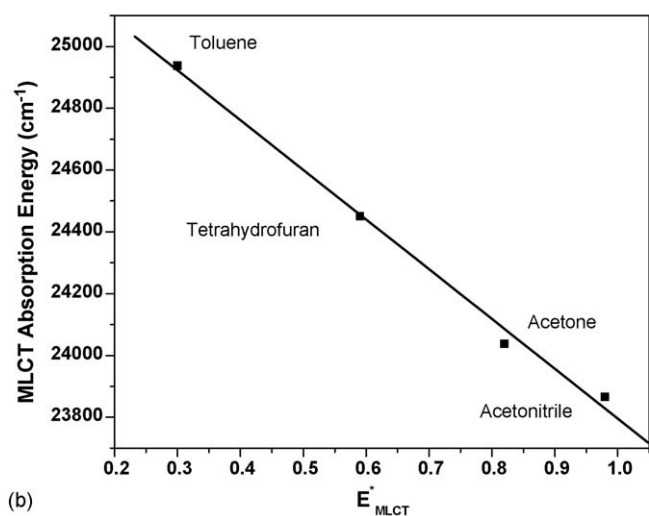
In the Pt(LL)(C \equiv CR)₂ structures, the low energy absorption bands show strong negative solvatochromism indicative of their polar ground states [26–28]. DFT calculations estimate ground state dipole moments (μ_{gr}) of approximately 10.6 D in Pt(bpy)(C \equiv CPh)₂, the vector of which directly opposes the direction of the charge transfer transition [28]. This is expected to lead to excited state dipole moments (μ_{ex}) close to or equal to zero. Although this result has been confirmed in a structurally related Pt(diimine)(dithiolate) using transient direct current photoconductivity (TDCP) [29], similar experiments have yet to be applied to the complexes which are the subject of this review. Since the solvent medium greatly influences ground state properties, solvent dielectric may be used to systematically tune the oxidation potential of the Pt(II) metal center in these complexes, reminiscent of ruthenium(II) polypyridine complexes bearing ancillary cyanide ligands [30,31]. An unusual preliminary observation in our laboratory demonstrates that a prototype [Pt(LLL)(C \equiv CR)]⁺ structure, **4**, exhibits positive solvatochromic behavior, Fig. 2b. The data obtained for the negatively solvatochromic **2** is included for comparison in Fig. 2a. In both instances, Lees E*_{MLCT} parameters [32] were used for each of the solvents in the study and excellent correlation coefficients were obtained for both molecules. Since the data is preliminary we do not wish to speculate on the origin of the positive solvatochromism in **4** at this time. These different medium effects are important to recognize when designing photophysical experiments and should to be accounted for when interpreting data. The remaining portions of this contribution examine the unique excited state properties and dynamics of several different mononuclear Pt(II) polyimine acetylides.

4. Photoluminescence properties

Fig. 3 displays the photoluminescence spectra of compounds **1–4** measured in CH₂Cl₂ at room temperature under optically dilute conditions. Upon photoexcitation into their respective charge transfer transitions, complexes **1–4** exhibit broad and structureless photoluminescence over a region spanning 500–750 nm. The large Stokes shift, relatively long lifetime and



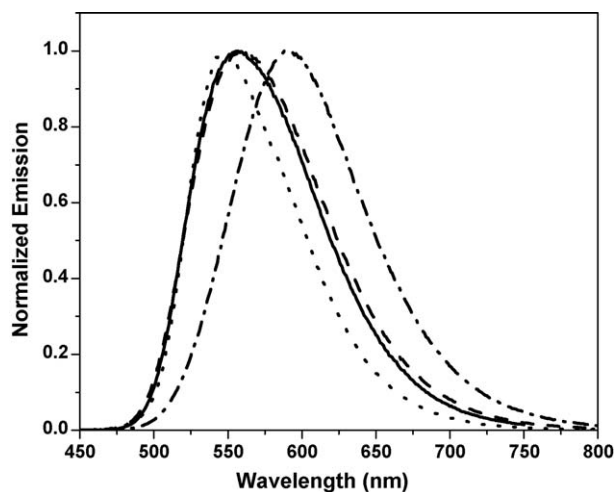
(a)



(b)

Fig. 2. Solvatochromic behavior of compounds **2** (a) and **4** (b).

susceptibility to quenching by dioxygen, suggest that the photoluminescence emanates from a triplet charge transfer excited state [18–20,22,27,28,33]. All excitation spectra were largely superimposable with corresponding absorption spectra at all wavelengths above 300 nm and were completely invariant to the emission monitoring wavelength. Table 1 summarizes the absorption and emission maxima for complexes **1–4** along with lifetimes and quantum yields. Importantly, the emission spectra

Fig. 3. Emission spectra of **1** (solid line), **2** (dashed line), **3** (dotted line) and **4** (dashed–dotted line) in CH_2Cl_2 .

of **1–4** are symmetrically quenched in all solvents investigated when the solution environment changes from argon-purged to air-saturated suggesting that an emission manifold comprised of one state or two closely lying states configurationally mixed or in rapid thermal equilibrium [28]. In all cases the emission intensity decays were well modeled by single-exponential kinetics and recovered lifetimes were constant along the entire emission profile. The excited state lifetimes were measured under optically dilute conditions where the measured intensity decays were invariant to the chromophore concentration ($\sim 10^{-5}$ M).

The Eisenberg and Schanze research groups have established energy gap law correlations in various $\text{Pt}(\text{LL})(\text{C}\equiv\text{CR})_2$ structures [18,19]. Systematic energy gap relationships have not been widely established in the terpyridyl systems to the best of our knowledge [20]. The coordinative unsaturation in the square planar $\text{Pt}(\text{II})$ complexes enables a variety of potential quenching processes by other $\text{Pt}(\text{II})$ molecules in solution as well as solvents. For example, these compounds are known to undergo self-quenching, displaying linear Stern–Volmer kinetics once a critical concentration is exceeded [34]. We investigated compound **4** in a concentration range up to 650 μM in CH_3CN . Over this range there is no evidence for ground state aggregation as indicated by Beer's Law behavior of the absorption spectra. Even though the periphery was designed to inhibit intermolecular self-quenching, complex **4**, bearing *tert*-butyl groups on

Table 1
Photophysical data for complexes **1–4** at room temperature^a

Compound	λ_{abs}^b (nm)	λ_{em}^b (nm)	τ_{em}^c (μs)	Φ_{em}^c	k_{r}^d (s^{-1})	k_{nr}^e ($\times 10^5 \text{ s}^{-1}$)
(1) $\text{Pt}(\text{dbbpy})(\text{CC}-t\text{Bu})_2$	403	557	1.06	0.48	4.5×10^5	4.9
(2) $\text{Pt}(\text{dbbpy})(\text{CC}-\text{Ph})_2$	396	562	1.36	0.34	2.5×10^5	4.8
(3) $[\text{Pt}(t\text{Bu}_3\text{tpy})(\text{CC}-t\text{Bu})]\text{ClO}_4$	408, 430	548	2.2	0.17	7.7×10^4	3.8
(4) $[\text{Pt}(t\text{Bu}_3\text{tpy})(\text{CC}-\text{Ph})]\text{ClO}_4$	411, 467	592	2.9	0.10	3.4×10^4	3.1

^a Optically dilute argon-degassed CH_2Cl_2 solutions.

^b Absorption and emission maxima, ± 2 nm.

^c PL quantum yields and intensity decays, $\pm 5\%$.

^d $k_{\text{r}} = \Phi/\tau$.

^e $k_{\text{nr}} = (1 - \Phi)/\tau$.

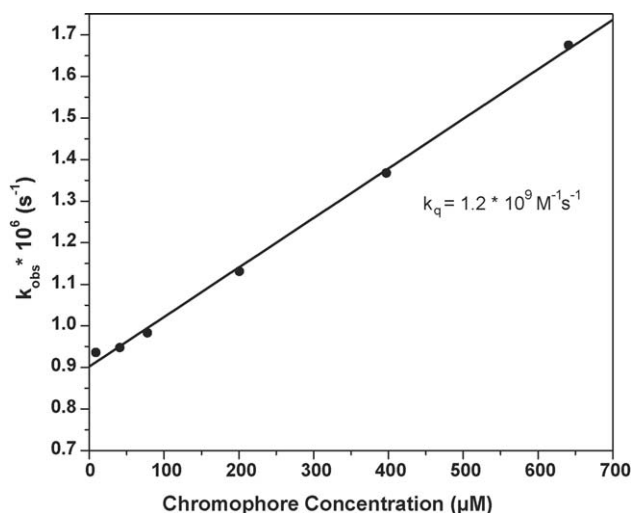


Fig. 4. The rates of emission decay of compound **4** in CH_3CN as a function of chromophore concentration.

the terpyridine ligand, undergoes dynamic self-quenching with a rate constant of $1.2 \times 10^9 \text{ M}^{-1} \text{ s}^{-1}$, Fig. 4. In many recent studies, the polyimine ligand purposely bears bulky *tert*-butyl substituents to minimize intermolecular quenching processes associated with ligand π -stacking and metal–metal interactions. It is important to note that in most instances that significant self-quenching takes place at relatively large concentrations ($>100 \mu\text{M}$) much larger than that utilized in typical excited state lifetime and quantum yield measurements. These dynamic processes and their photophysical consequences have been discussed in a recent review by Fleeman and Connick [35].

We currently have good evidence that Lewis basic solvents such as CH_3CN dynamically quench the photoluminescence of various molecules in both structural classes. It is most clearly observed in alkylacetylide structures in $\text{Pt}(\text{LL})(\text{C}\equiv\text{CR})_2$ systems and is readily observed in both alkyl- and arylacetylide substituted terpyridyl structures. For example, **4** is dynamically quenched by CH_3CN which is adequately described as a pseudo-first-order process with a rate constant of $2.0 \times 10^5 \text{ M}^{-1} \text{ s}^{-1}$, Fig. 5. The rates of emission decays ($k_{\text{obs}} = 1/\tau$) for both **3** and **4** were satisfactorily modeled by the modified Stern–Volmer equation ($k_{\text{obs}} = k_q[\text{CH}_3\text{CN}] + k_0$) and acetonitrile-quenching rate constants k_q have been estimated. It was found that quenching rate constant by acetonitrile for complex **4** ($2.0 \times 10^5 \text{ M}^{-1} \text{ s}^{-1}$) is almost an order of magnitude smaller than that of **3** ($1.25 \times 10^6 \text{ M}^{-1} \text{ s}^{-1}$), Fig. 5. One possibility is that in structure **4**, the “hole” generated in the excited state is more widely delocalized (over the Pt atom and the phenyl rings) whereas in **3**, charge transfer excitation would lead to more localized “hole” density on the metal center. This would render the metal center in **3** more susceptible to nucleophilic attack by Lewis basic solvents which may account for the order of magnitude increase in the observed rate constant. At the present time we do not wish to further speculate on the origin of the excited state quenching but note that these findings are similar to what McMillin and co-workers have discovered in $[\text{Pt}(\text{LLL})\text{Cl}]^+$ systems [36].

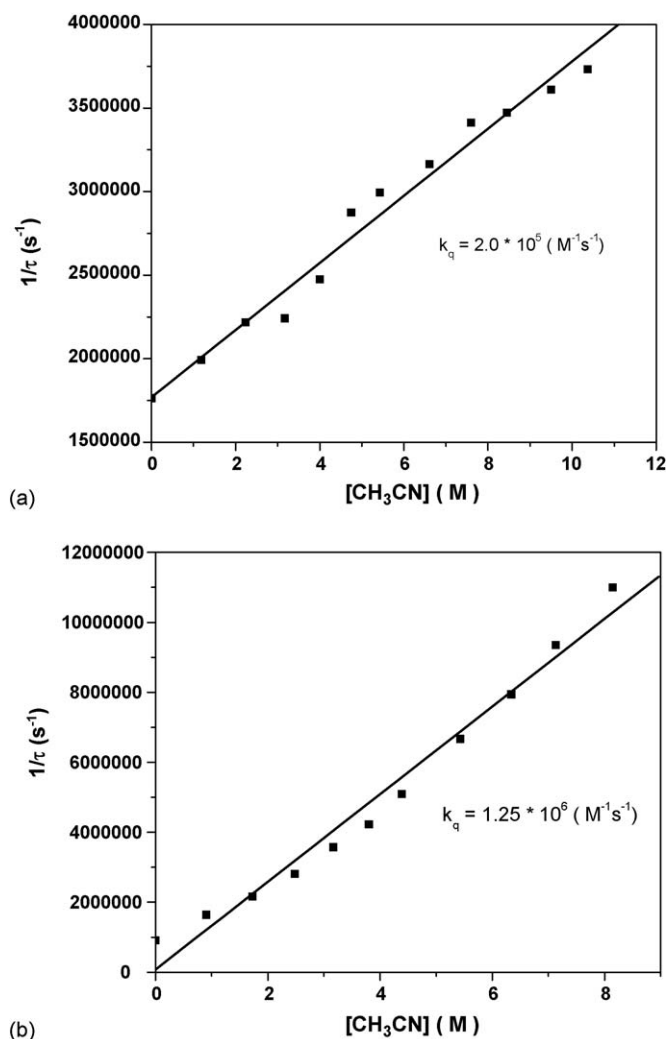


Fig. 5. The rates of emission decay of (a) **4** and (b) **3** in CH_2Cl_2 as a function of CH_3CN concentration.

Most of the work on $\text{Pt}(\text{LL})(\text{C}\equiv\text{CR})_2$ and $[\text{Pt}(\text{LLL})(\text{C}\equiv\text{CR})]^+$ to date has focused on excited state behavior that is largely dictated by decay of the triplet charge transfer level in these molecules, yielding charge transfer based luminescence as illustrated in Fig. 3. However, if the $^3\pi-\pi^*$ states associated with the acetylide units are strategically placed below the $^3\text{MLCT}$ level, then the charge transfer states can be used to internally sensitize the production of one of the triplet arylacetylide moieties present in the structure [27,28,33]. With the aid of the internal heavy atom, acetylide ligand-localized long lifetime room temperature phosphorescence can be derived. This is straightforwardly observed in our original prototype system $\text{Pt}(\text{dbbpy})(\text{C}\equiv\text{C}-\text{pyrene})_2$ (**5**) [27], as well as in $\text{Pt}(\text{dbbpy})(\text{C}\equiv\text{C}-\text{anthracene})_2$ (**6**) [37] and $\text{Pt}(\text{dbbpy})(\text{CC}-\text{perylene})_2$ (**7**) [37] [$\text{C}\equiv\text{C}-\text{pyrene}$ = 1-ethynylpyrene, $\text{C}\equiv\text{C}-\text{anthracene}$ = 9-ethynylanthracene, $\text{CC}-\text{perylene}$ = 3-ethynylperylene], where the charge transfer excited states were used to internally sensitize the production of the $^3\pi-\pi^*$ excited state localized on one of the aromatic acetylide moieties *trans* to the diimine system.

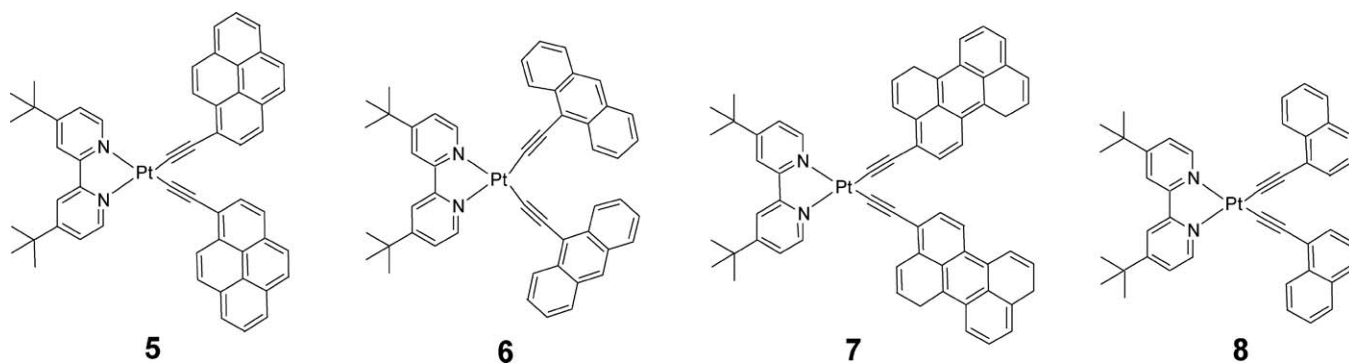


Fig. 6 presents the absorption spectra of **5–7** in CH_2Cl_2 . The arylacetylide chromophores are responsible for the structured $\pi-\pi^*$ transitions between 325 and 500 nm. The shift of the $\pi-\pi^*$ transitions to lower energy in going from $\text{C}\equiv\text{C}$ –pyrene to the $\text{C}\equiv\text{C}$ –perylene is due to more extended conjugation in the series. The visible absorption band near 450 nm observed for **5** and **6** are attributed to the Pt $d\pi \rightarrow \pi^*$ dbbpy MLCT transitions and, although red-shifted, are qualitatively similar to that of **2** (Fig. 1a). The $^1\text{MLCT}$ band in **7** is not distinguishable under the broad and structured perylene-localized $\pi-\pi^*$ transitions due to the sheer intensity of those transitions. In this instance, the perylene singlet and triplet states are located at much lower in energy than the corresponding pyrenylacetylide and anthracenylacetylide compounds, resulting in the overlap of $\pi-\pi^*$ and charge transfer transitions, Fig. 6. The red shift in the MLCT absorption band position going from **2** to **5–7** is most likely reflecting an increase of σ -donation of arylacetylide electron density to the Pt(II) center in this series of compounds. There are also undoubtedly contributions resulting from stronger arylacetylide ligand mixing in the low energy (ML)LCT transition.

Fig. 7 depicts room temperature phosphorescence spectra in deaerated dichloromethane of compounds **5–7**. It is established that luminescence in **2** is attributed to the charge transfer

manifold [18,19,27,28], whereas the emission from **5**, **6**, and **7** are substantially red-shifted, structured, and relatively sharp in comparison. Due to the extensive overlap of the anthraceneacetylide and peryleneacetylide $\pi \rightarrow \pi^*$ and $d\pi(\text{Pt}) \rightarrow \pi^*$ (diimine) absorption bands, excitation at low energy (480 and 488 nm, respectively) results in both fluorescence and phosphorescence emanating from corresponding arylacetylide ligands, however, only the phosphorescence in each case is displayed in Fig. 7. The observed phosphorescence from the ethynylperylene moieties is relatively weak, nevertheless a vibronic progression is quite distinguishable with a maximum around 882 nm in the near-IR.

Another notable compound prepared in our laboratory, $\text{Pt}(\text{dbbpy})(\text{C}\equiv\text{C}\text{-nap})_2$ (**8**), where $\text{C}\equiv\text{C}\text{-nap}$ is naphthylacetylide, displays solvent-dependent excited state behavior [28]. In this case, the emerging photoluminescence can be considered predominantly charge transfer like in non-polar solvents and more naphthylacetylide localized in higher polarity media, Fig. 8. The substantial solvent influence is also readily observed in nanosecond flash photolysis experiments where the excited state difference spectra markedly change as a function of solvent. This particular study stresses the importance and necessity of transient absorption measurements in understanding the nature of the lowest excited states in these complexes.

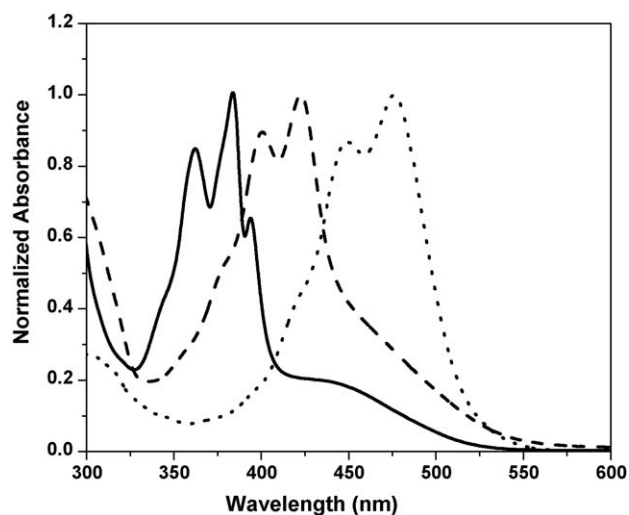


Fig. 6. Absorption spectra of **5** (solid line), **6** (dashed line) and **7** (dotted line) in CH_2Cl_2 .

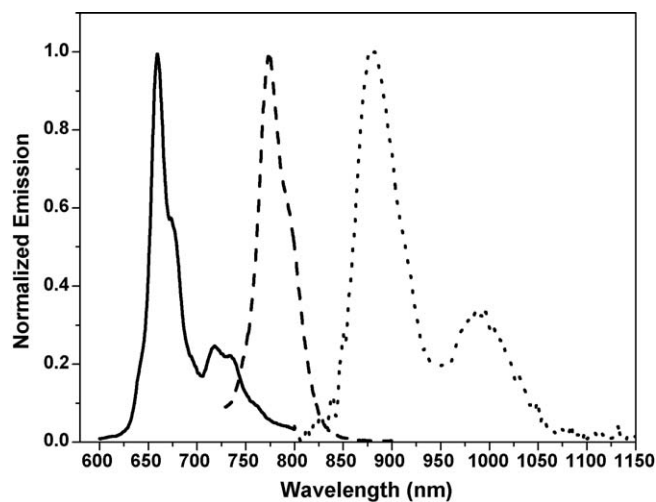


Fig. 7. Room temperature phosphorescence spectra of **5** (solid line), **6** (dashed line) excited at 480 nm and **7** (dotted line) excited at 488 nm in deaerated CH_2Cl_2 .

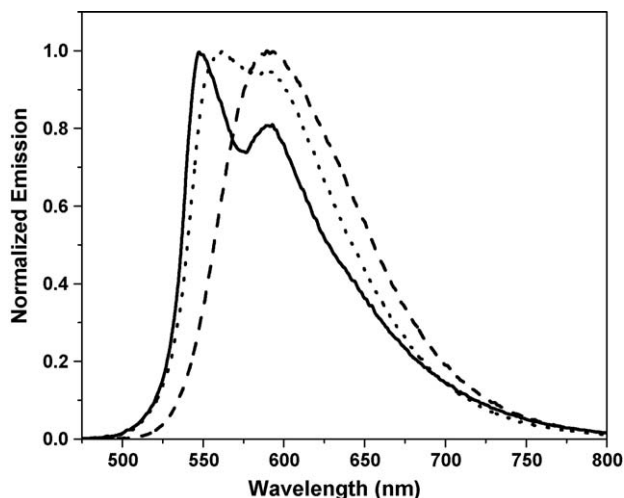


Fig. 8. Static photoluminescence spectra of **8** in CH_3CN (solid line), CH_2Cl_2 (dotted line) and toluene (dashed line).

5. Excited state absorption spectrometry

5.1. Supra-nanosecond spectrometry

While luminescence spectroscopy has been widely applied to the study of Pt(II) polyimine acetylides, there have only been a handful of transient absorption investigations [2,3,19,26–28,33,38–40] along with a single time-resolved infrared study [19]. The latter can be easily understood in terms of the low IR-absorption cross-sections uniformly observed for acetylide stretching frequencies, rendering their detection rather difficult. Regardless, a few Pt(II) diimine acetylides have been studied using nanosecond step-scan FTIR. In the same manuscript, the nanosecond excited state absorption spectra of several Pt(II) diimine acetylides were also reported [19]. The excited state absorptions were assigned as resulting from the MLCT excited state with contributions from ground state bleaching, reduced diimine ligand, and oxidized metal center. A difficult facet of these excited states is that one cannot properly correlate excited state absorptions directly to ground state oxidations and reductions since these compounds are uniformly unstable to spectroelectrochemical measurements. Transient features associated with the charge transfer excited states or electron transfer products are readily identifiable, but their precise origins have been largely speculative. With the wealth of new information provided by recent electronic structure calculations [22,25], the charge transfer excited states can be considered to be composed of a hole delocalized over the Pt center and the acetylide ligand(s) framework with the electron localized on the polyimine ligand. Therefore, the excited state absorptions in the charge transfer state will reflect all of these contributions in addition to potential transitions between these moieties. Fig. 9 presents the transient difference spectra of **3** and **4** in degassed CH_2Cl_2 . Recall that the σ -donor strength of phenylacetylide and *t*-butylacetylide are essentially the same and the remaining portions of each molecule are constant. While there are similarities in the excited state spectra, differences are also readily apparent which must stem from differences in the electronic structure of the photo-created

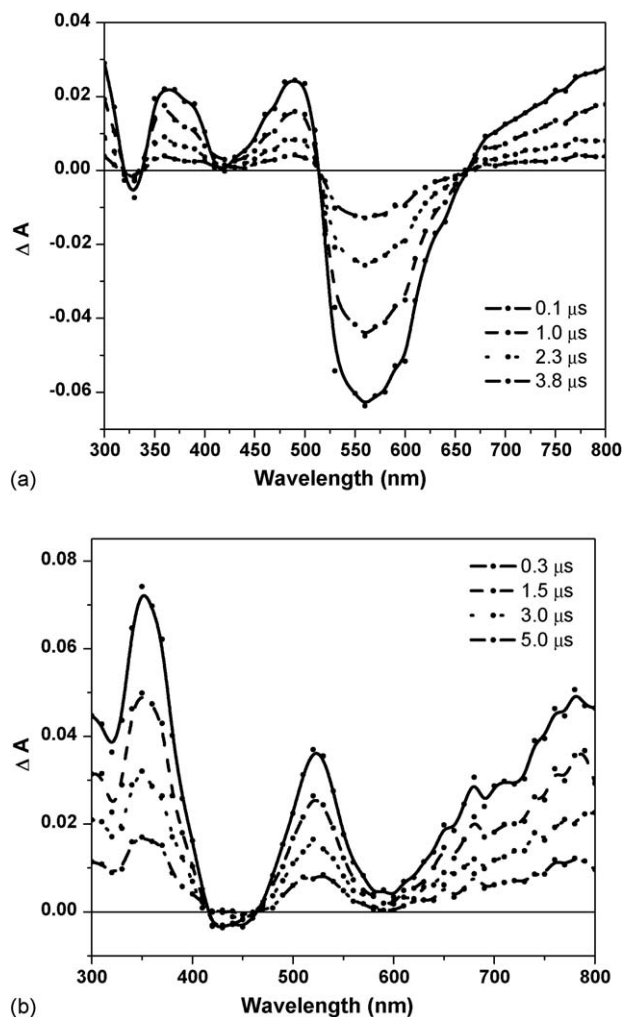


Fig. 9. Excited state absorption difference spectra of (a) **3** and (b) **4** in CH_2Cl_2 following 416 nm excitation (3 mJ/pulse). The delay times are specified on each spectrum. The apparent bleach between 500 and 650 nm in (a) is due to strong sample photoluminescence.

hole. To test this idea, we prepared the related Ru(II) structure $[\text{Ru}(\text{tBu}_3\text{tpy})_2]^{2+}$, where ultrafast transient absorption measurements yield a difference spectrum ($\tau = 115$ ps) whose strongest transiently absorbing component is the *t*Bu₃tpy radical anion, Fig. 10 [41]. Clearly, this transient is partially responsible for the highest energy feature in the Pt(II) complexes but cannot account for the lower energy bands that extend beyond our instrument range into the near-IR.

To better understand what gives rise to these intense transient absorptions without the benefit of spectroelectrochemistry, we performed transient trapping experiments on the excited states **3** and **4**. Briefly, both complexes were subjected to flash photolysis in the presence of the reductive quencher diazabicyclooctane (DABCO, $E_{1/2} = +0.57$ V versus NHE) [42] whose radical cation is largely spectroscopically silent over the absorption range of interest, $\epsilon = 1500 \text{ M}^{-1} \text{ cm}^{-1}$ at 470 nm [43]. DABCO has the added advantage of reversible cyclic voltammetry, therefore charge recombination occurs readily with each platinum complex's reduced ground state via second-order equal-concentration kinetics. Experimentally, we see no buildup of

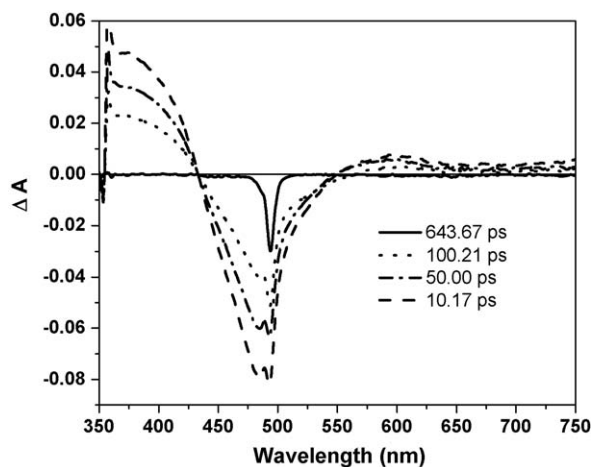


Fig. 10. Ultrafast transient absorption difference spectra of $[\text{Ru}(\text{tBu}_3\text{tpy})_2](\text{PF}_6)_2$ in CH_2Cl_2 following 490 nm excitation. The delay times are specified on the graph. The sharp feature present at all delay times at 490 nm is from the pump laser.

permanent photochemical products in the transient absorption measurements and this facilitates straightforward spectroscopic assignments. Stern–Volmer analysis of the emission lifetimes as a function of DABCO concentration confirmed strong pseudo-first-order quenching with rate constants approaching the diffusion limit for both molecules in CH_2Cl_2 . Fig. 11 presents the excited state absorption difference spectrum of **4** measured in the presence of DABCO following 355 nm pulsed laser excitation. Most of the strong transient absorption features across the visible spectrum and towards the near-IR disappear upon reductive quenching. Therefore, the transiently produced “hole” in the charge transfer excited state must play a significant role in governing the position and intensity of the absorption transients. The only transient feature that remains in the near visible can be assigned to reduced tBu_3tpy [40,41], whose absorption intensity is minor in comparison to that of the entire charge transfer excited state, even at the peak $\text{tBu}_3\text{tpy}^{\bullet-}$ wavelengths. This simple experiment supports the notion that the majority of

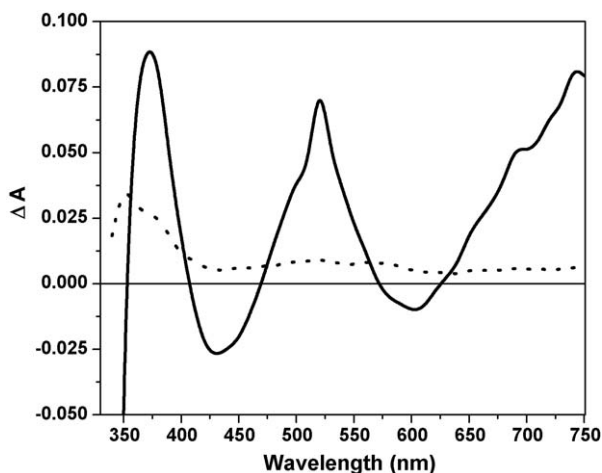


Fig. 11. Excited state absorption difference spectrum of **4** in the presence of DABCO immediately following a 355 nm laser pulse (solid line) and after significant reductive quenching (dashed line).

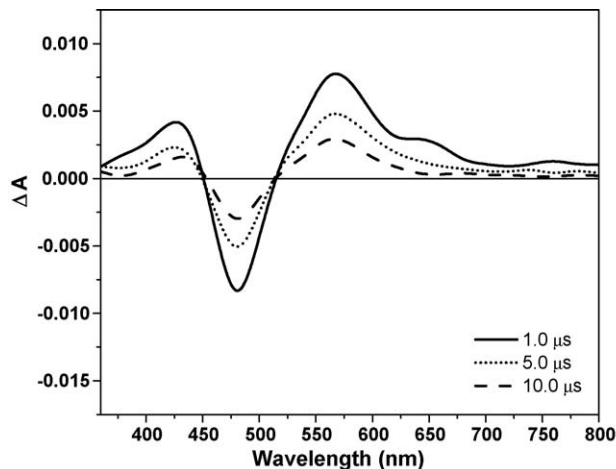


Fig. 12. Transient absorption difference spectrum of **7** in deaerated MTHF following 416 nm pulsed laser excitation.

the absorption transients most likely have their origin in excited state charge transfer transitions (perhaps LLCT and/or LMCT) to and/or from the delocalized “hole”. In other words, the difference spectra are not derived solely from the combination of redox products that one usually probes using ground state spectroelectrochemistry. Therefore, with better understanding of the delocalized “hole”, we anticipate that optical protection materials based on these structures can be substantially improved.

Nanosecond laser flash photolysis experiments are also powerful for identifying the production of acetylide ligand-localized triplet states in these molecules. For example, **5** and **7** exhibit strong absorptions centered near 530 and 570 nm, respectively, which decay by first order kinetics to their ground states. The data for compound **5** and its associated phosphine-bearing model system have already been published and the transient at 530 nm assigned to the triplet state of pyrenylacetylide [27,38]. Fig. 12 displays the transient absorption difference spectra obtained for $\text{Pt}(\text{dbbpy})(\text{C}\equiv\text{C}\text{--}\text{perylene})_2$ following a 416 nm laser flash. The positive OD bands at 425 and 570 nm are assigned to peryleneacetylide-localized triplet-to-triplet absorptions and the bleach is associated with the bleaching of the peryleneacetylide $\pi\text{--}\pi^*$ ground state transitions [37]. The fact that the perylene-localized singlet absorption bands bleach and recover on the same microseconds time scale ($\tau = 8.35 \mu\text{s}$) as the other features, supporting the triplet state assignment of the transient absorptions.

5.2. Ultrafast transient absorption spectrometry

While the number of Pt(II) chromophores have expanded significantly over the past decade, their sub-nanosecond excited state dynamics remain largely unexplored, with three exceptions. One study by McGarrah and Eisenberg described the detection of charge-separated products in electron transfer donor-acceptor dyads at initial delay times of 100 ps following a 20 ps laser pulse [26]. Intramolecular electron transfer processes were also studied between platinum(II) terpyridyl complex coupled to a porphyrin through an arylacetylide bridge [39].

Excitation of the porphyrin leads to rapid electron transfer with the Pt(II) complex followed by ultrafast charge recombination. Another investigation is from our laboratory where excited state evolution of the charge transfer excited state was examined along with its subsequent depopulation resulting from potentially strong interactions with arylacetylide-localized ^3IL states [38]. The ultrafast excited state dynamics of three structurally related platinum(II) complexes were investigated using femtosecond transient absorption spectrometry in 2-methyltetrahydrofuran. It has already been stated that **2** has a lowest metal-to-ligand charge transfer ($^3\text{MLCT}$) excited state while the multichromophoric **5** contains the MLCT state, but possesses a lowest intraligand (^3IL) excited state localized on one of the $\text{C}\equiv\text{C}$ –pyrenyl units. *Trans*-Pt(PBu₃)₂(C≡C–pyrene)₂ served as a model system that provided a good representation of the $\text{C}\equiv\text{C}$ –pyrene-localized ^3IL state in a Pt(II) complex lacking the MLCT excited state. Following 400 nm excitation, the formation of the $^3\text{MLCT}$ excited state in **2** is complete within 200 ± 40 fs and intersystem crossing to the ^3IL excited state in *trans*-Pt(PBu₃)₂(C≡C–pyrene)₂ occurs with a time constant of 5.4 ± 0.2 ps. Selective excitation into the low energy MLCT bands in **5** ($\lambda_{\text{ex}} = 480$ nm) leads to the formation of the pyrene-localized ^3IL excited state in 240 ± 40 fs, suggesting ultrafast wire-like energy migration in this molecule. Indiscriminant excitation of **5** at 400 nm, which predominately promotes the pyrenylacetylide π – π^* singlet transition, leads to exactly the same time constant within experimental error for the formation of the ^3IL excited state, 210 ± 40 fs. The kinetic data contend that the presence of the MLCT states in **5** markedly accelerates the formation of the triplet state of the pendant pyrenylacetylide ligand. In essence, the triplet sensitization process is kinetically faster than pure intersystem crossing in *trans*-Pt(PBu₃)₂(C≡C–pyrene)₂ as well as vibrational relaxation in the MLCT excited state of **2**. The kinetic results may indeed arise from extremely rapid triplet energy transfer in **5**. However, given the similarities in the time constants for ^3IL state formation using 400 and 480 nm excitation, intersystem crossing in the pyrenylacetylide chromophore is somehow accelerated in **5**. Therefore the ultrafast nature of the ^3IL formation time constants could result from strong mixing of the MLCT triplet state with that of the pyrenylacetylide triplet. This would enable enhanced spin–orbit coupling and could account for the experimental observations. Similar arguments have been used to describe the phosphorescence emanating from bodipy (4,4-difluoro-4-bora-3a,4a-diaza-*s*-indacene) dyes when this species is appended to a Ru(II) terpyridine chromophore [44]. These results are potentially important for the design of chromophores intended to reach their lowest excited state on sub-picosecond time scales and advocates the likelihood of wire-like behavior in triplet-triplet energy transfer in these molecules. Our laboratory continues to explore ultrafast dynamics in the title Pt(II) complexes, seeking a more thorough understanding of energy migration dynamics in these structures.

6. Concluding remarks

Although the primary motivation for research in this area largely stems from the potential applications of these chro-

mophores across a variety of disciplines, the fact remains that there are many interesting questions remaining and several lines of investigation worth further exploration. This contribution was intended to outline current work in the field related predominately to the photophysical processes in bipyridyl and terpyridyl platinum(II) acetylides. Even within this seemingly small group of related molecular structures, there exists an enormous complexity arising from the strong participation of the acetylide ligand(s) in the ground and excited states of these molecules. The extent of orbital mixing taking place is readily observed experimentally in ground state spectra and theoretically using density functional methods. Such intricacies are not usually observed in coordination compounds displaying clear cut MLCT-type photophysics, leading to the most appropriate charge transfer designation in these systems, namely (ML)LCT. The photoluminescence of the Pt(II) acetylides is noteworthy and can take the form of “pure” triplet charge transfer like or “pure” triplet acetylide ligand localized in character, depending upon the choice of polyimine and acetylide ligand(s). It has also been shown that the photophysics can fall between those two extremes, for example compound **8**, can be best described as admixtures of $^3\text{MLCT}$ and ^3IL states, systematically tunable between both by varying solvent polarity. Transient absorption methods have been extremely useful in identifying intermediates and products generated in both intra- and intermolecular energy and electron transfer reactions utilizing platinum(II) acetylides. Although there are only a handful of reports to date, ultrafast kinetic methods clearly have a promising future in exploring the complexities resulting from the strong orbital mixing in these structures. The horizon appears bright for continued fundamental scientific exploration of platinum acetylides in addition to their widespread applications in photonics, medicine, nanomaterials, and catalysis.

Acknowledgements

We gratefully acknowledge the NSF (CAREER Award CHE-0134782), the AFOSR (FA9550-05-1-0276), the ACS-PRF (44138-AC3 and 36156-G6), and Bowling Green State University (Technology Innovation Enhancement Award) for their generous support of our own research projects relevant to this review. All transient absorption measurements described in this review were performed in the Ohio Laboratory for Kinetic Spectrometry at BGSU. We thank Dr. Albert Okhrimenko for acquiring the near-IR emission spectrum of compound **7** and Alexander D. Tregubov for the preparation/characterization of [Ru(*t*Bu₃tpy)₃](PF₆)₂.

References

- [1] C.W. Chan, L.K. Cheng, C.M. Che, *Coord. Chem. Rev.* 132 (1994) 87.
- [2] W. Sun, Z.-X. Wu, Q.-Z. Yang, L.-Z. Wu, C.-H. Tung, *Appl. Phys. Lett.* 82 (2003) 850.
- [3] F. Guo, W. Sun, Y. Liu, K. Schanze, *Inorg. Chem.* 44 (2005) 4055.
- [4] S.-C. Chan, M.C.W. Chan, Y. Wang, C.-M. Che, K.-K. Cheung, N. Zhu, *Chem. Eur. J.* 7 (2001) 4180.
- [5] D. Zhang, L.-Z. Wu, Q.-Z. Yang, X.-H. Li, L.-P. Zhang, C.-H. Tung, *Org. Lett.* 5 (2003) 3221.

- [6] Y. Yang, D. Zhang, L.-Z. Wu, B. Chen, L.-P. Zhang, C.-H. Tung, J. Org. Chem. 69 (2004) 4788.
- [7] D. Zhang, L.-Z. Wu, L. Zhou, X. Han, Q.-Z. Yang, L.-P. Zhang, C.-H. Tung, J. Am. Chem. Soc. 126 (2004) 3440.
- [8] Q.-Z. Yang, L.-Z. Wu, H. Zhang, B. Chen, Z.-X. Wu, L.-P. Zhang, C.-H. Tung, Inorg. Chem. 43 (2004) 5195.
- [9] Q.-Z. Yang, Q.-X. Tong, L.-Z. Wu, Z.-X. Wu, L.-P. Zhang, C.-H. Tung, Eur. J. Inorg. Chem. (2004) 1948.
- [10] V.W.-W. Yam, R.P.-L. Tang, K.M.-C. Wong, K.-K. Cheung, Organometallics 20 (2001) 4476.
- [11] W. Lu, C.W. Chan Michael, N. Zhu, C.-M. Che, Z. He, K.-Y. Wong, Chem. Eur. J. 9 (2003) 6155.
- [12] D.-L. Ma, T.Y.-T. Shum, F. Zhang, C.-M. Che, M. Yang, Chem. Commun. (2005) 4675.
- [13] K.M.-C. Wong, W.-S. Tang, B.W.-K. Chu, N. Zhu, V.W.-W. Yam, Organometallics 23 (2004) 3459.
- [14] K.D. Hodges, J.V. Rund, Inorg. Chem. 14 (1975) 525.
- [15] V.Y. Kukushkin, A.J.L. Pombeiro, C.M.P. Ferreria, L.I. Elding, Inorg. Synth. 33 (2002).
- [16] K. Sonogashira, Y. Fujikura, N. Toyoshima, S. Takahashi, N. Hagihara, J. Organomet. Chem. 145 (1978) 101.
- [17] S.L. James, M. Younus, P.R. Raithby, J. Lewis, J. Organomet. Chem. 543 (1997) 233.
- [18] M. Hissler, W.B. Connick, D.K. Geiger, J.E. McGarrah, D. Lipa, R.J. Lachicotte, R. Eisenberg, Inorg. Chem. 39 (2000) 447.
- [19] C.E. Whittle, J.A. Weinstein, M.W. George, K.S. Schanze, Inorg. Chem. 40 (2001) 4053.
- [20] Q.-Z. Yang, L.-Z. Wu, Z.-X. Wu, L.-P. Zhang, C.-H. Tung, Inorg. Chem. 41 (2002) 5653.
- [21] V.W.-W. Yam, K.M.-C. Wong, N. Zhu, Angew. Chem. Int. Ed. 42 (2003) 1400.
- [22] F. Hua, S. Kinayyigit, J.R. Cable, F.N. Castellano, Inorg. Chem. 44 (2005) 471.
- [23] V.W.-W. Yam, Chem. Commun. (2001) 789.
- [24] S.D. Cummings, R. Eisenberg, J. Am. Chem. Soc. 118 (1996) 1949.
- [25] X. Zhou, H.-X. Zhang, Q.-J. Pan, B.-H. Xia, A.-C. Tang, J. Phys. Chem. A 109 (2005) 8809.
- [26] J.E. McGarrah, R. Eisenberg, Inorg. Chem. 42 (2003) 4355.
- [27] I.E. Pomestchenko, C.R. Luman, M. Hissler, R. Ziessel, F.N. Castellano, Inorg. Chem. 42 (2003) 1394.
- [28] I.E. Pomestchenko, F.N. Castellano, J. Phys. Chem. A 108 (2004) 3485.
- [29] F.W.M. Vanhelmont, R.C. Johnson, J.T. Hupp, Inorg. Chem. 39 (2000) 1814.
- [30] F. Scandola, M.T. Indelli, Pure Appl. Chem. 60 (1988) 973.
- [31] C.J. Timpson, C.A. Bignozzi, B.P. Sullivan, E.M. Kober, T.J. Meyer, J. Phys. Chem. 100 (1996) 2915.
- [32] D.M. Manuta, A.J. Lees, Inorg. Chem. 22 (1983) 3825.
- [33] K. Haskins-Glusac, I. Ghiviriga, K.A. Abboud, K.S. Schanze, J. Phys. Chem. B 108 (2004) 4969.
- [34] W.B. Connick, D. Geiger, R. Eisenberg, Inorg. Chem. 38 (1999) 3264.
- [35] W.L. Fleeman, W.B. Connick, Comment Inorg. Chem. 23 (2002) 205.
- [36] D.K.C. Tears, D.R. McMillin, Coord. Chem. Rev. 211 (2001) 195.
- [37] I.E. Pomestchenko, Ph.D. Dissertation, Bowling Green State University, 2004.
- [38] E.O. Danilov, I.E. Pomestchenko, S. Kinayyigit, P.L. Gentili, M. Hissler, R. Ziessel, F.N. Castellano, J. Phys. Chem. A 109 (2005) 2465.
- [39] C. Monnereau, J. Gomez, E. Blart, F. Odobel, S. Wallin, A. Fallberg, L. Hammarstroem, Inorg. Chem. 44 (2005) 4806.
- [40] S. Chakraborty, T.J. Wadas, H. Hester, C. Flaschenreim, R. Schmehl, R. Eisenberg, Inorg. Chem. 44 (2005) 6284.
- [41] R.M. Berger, D.R. McMillin, Inorg. Chem. 27 (1988) 4245.
- [42] W. Hub, S. Schneider, F. Dorr, J.D. Oxman, F.D. Lewis, J. Am. Chem. Soc. 106 (1984) 701.
- [43] T. Shida, Y. Nosaka, T. Kato, J. Phys. Chem. 82 (1978) 695.
- [44] M. Galletta, S. Campagna, M. Quesada, G. Ulrich, R. Ziessel Chem. Commun. (2005) 4222.